

Intrastratial CERE-120 (AAV-Neurturin) protects striatal and cortical neurons and delays motor deficits in a transgenic mouse model of Huntington's disease

Shilpa Ramaswamy^a, Jodi L. McBride^{a,c}, Ina Han^a, Elizabeth M. Berry-Kravis^d, Lili Zhou^d, Christopher D. Herzog^b, Mehdi Gasmi^b, Raymond T. Bartus^b, Jeffrey H. Kordower^{a,*}

^a Department of Neurological Sciences, Rush University Medical Center, 1735 West Harrison Street, Suite 300, Chicago, IL 60612, USA

^b Ceregene Inc., 9381 Judicial Drive, Suite 130, San Diego, CA 92121, USA

^c Oregon National Primate Research Center, Division of Neuroscience, 505 NW 185th Avenue, Beaverton, OR 97006, USA

^d Department of Pediatric Neurology, Rush University Medical Center, 1725 West Harrison Street, Suite 718, Chicago, IL 60612, USA

ARTICLE INFO

Article history:

Received 21 September 2008

Revised 5 December 2008

Accepted 9 December 2008

Available online 25 December 2008

Keywords:

Huntington's disease

N171-82Q

Neurturin

CERE-120

Gene therapy

Transgenic mouse model

AAV2

ABSTRACT

Members of the GDNF family of ligands, including neurturin (NTN), have been implicated as potential therapeutic agents for Huntington's disease (HD). The present study examined the ability of CERE-120 (AAV2-NTN) to provide structural and functional protection in the N171-82Q transgenic HD mouse model. AAV2-NTN therapy attenuated rotorod deficits in this mutant relative to control treated transgenics ($p < 0.01$). AAV2-NTN treatment significantly reduced the number of transgenic mice that exhibited clasping behavior and partially restored their stride lengths (both $p < 0.05$). Stereological counts of NeuN-ir neurons revealed a significant neuroprotection in the striatum of AAV2-NTN treated relative to control treated transgenics ($p < 0.001$). Most fascinating, stereological counts of NeuN-labeled cells in layers V–VI of prefrontal cortex revealed that intrastratial AAV2-NTN administration prevented the loss of frontal cortical NeuN-ir neurons seen in transgenic mice ($p < 0.01$). These data indicate that gene delivery of NTN may be a viable strategy for the treatment of this incurable disease.

© 2008 Elsevier Inc. All rights reserved.

Introduction

Huntington's disease (HD) is an incurable, devastating neurodegenerative disorder caused by a mutation in the *IT15* gene and inherited in an autosomal dominant manner (The Huntington's Disease Collaborative Research Group, 1993). The mutation is a trinucleotide repeat expansion in exon 1 of the HD gene. These excessive repeats lead to the expression of a mutant huntingtin protein with an expanded glutamine stretch at the N-terminus. Mutant huntingtin is expressed throughout the brain but is preferentially toxic to striatal and cortical neurons. The extensive neurodegeneration in the brains of HD patients causes severe deficits in the motor, cognitive and personality domains. Unfortunately, there is no effective therapy for HD.

In the striatum, cell death occurs primarily in medium-sized spiny neurons that express γ -aminobutyric acid (GABA) and either substance P or enkephalin. These two populations of striatal neurons show variable vulnerability at different stages of HD (Reiner et al., 1988). In early stages, neurons that co-express enkephalin are preferentially lost, while in latter stages, those expressing substance P degenerate.

This striatal loss likely underlies the motor deficits seen in HD. Cortical degeneration is also a prominent pathological feature and likely mediates the deficits seen in higher order cognitive functions which can often be the more devastating clinical features of HD. Cell loss occurs in several layers of the cortex but is most prominent in layers III, V and VI (Hedreen et al., 1991; Selemon et al., 2004).

For decades, neurotrophic factors have been considered to have great potential for a variety of neurodegenerative diseases. Studies in animal models of HD suggest that several, neurotrophic factors including members of the glial cell line-derived neurotrophic factor family of ligands (GFL) (McBride et al., 2006; Perez-Navarro et al., 2000), the cytokines (Anderson et al., 1996; Emerich et al., 1997a) and the neurotrophins (Canals et al., 2004; Martinez-Serrano and Bjorklund, 1996) may have therapeutic potential for treating patients. Our group has recently demonstrated that adeno-associated viral vector serotype 2 (AAV2) delivery of the NTN gene, via CERE-120 protects striatal neurons from degeneration and rescues motor deficits in the 3NP rat model of HD (Ramaswamy et al., 2007). However, tests of potential efficacy and clinical utility, for HD should include genetic models of HD. One such transgenic model is the N171-82Q transgenic mouse. N171-82Q mice contain a human cDNA encoding for the N-terminal fragment of huntingtin (Schilling et al., 1999). This model expresses 82 polyglutamine repeats, a number that is clinically relevant, and models adult onset HD. These mice also

* Corresponding author. Fax: +1 312 563 3571.

E-mail address: jkordowe@rush.edu (J.H. Kordower).

Available online on ScienceDirect (www.sciencedirect.com).

exhibit a significant loss of NeuN-ir neurons within the striatum (McBride et al., 2006) and cortex, mimicking a state seen in patients. Mimicking another condition seen in patients, these mice have a reduced life-span ranging from 2.5–6 months of age. Indeed, we have previously demonstrated that viral delivery of GDNF preserved motor function and protected striatal NeuN-ir neurons using this model (McBride et al., 2006). In the present study, we tested a naturally-occurring structural and functional analog of GDNF, neurturin (NTN). As in the prior GDNF study, we employed gene therapy to deliver the protein using an AAV2 viral vector. The actual vector construct tested in this study was CERE-120, which has been widely published on recently (Gasmi et al., 2007; Marks, et al., 2008). Moreover, CERE-120 is a GMP-manufactured product that has been tested for long-term safety under GLP conditions and has gone through FDA and RAC review to advance into clinical trials where it has now been tested in approximately 50 Parkinson's patients without any serious side effects. Thus, the data collected with CERE-120 (AAV2-NTN) in the HD transgenic model facilitates the translation of a GFL neurotrophic factor far better, more realistically, and more rapidly than can occur with AAV-GDNF for patients with HD. Towards this end, the present series of experiments tests the hypothesis that intrastriatal administration of AAV2-NTN, delivered before the onset of symptoms, can help protect against loss of motor function, preserve striatal and cortical neurons and prolong life-span in N171-82Q transgenic mice.

Materials and methods

Animals

Adult N171-82Q breeding pairs were obtained from Jackson Laboratories and housed in the animal care facility at Rush University Medical Center. Mice were mated to establish a colony. All mice were maintained in a 12-hour light–dark cycle and given food and water *ad libitum*. All experiments were performed with Institutional Animal Care and Use Committee approval and according to both federal and institutional guidelines. PCR was performed to genotype all mice by using primers previously described (Schilling et al., 1999).

Experimental paradigm

The timeline for all procedures is presented in Fig. 1A. To study the efficacy of treatments, all mice underwent baseline behavioral testing at postnatal week 5 and then one week later received bilateral vector

or vehicle injections into the striatum. Subsequent behavioral tests were conducted weekly until the end of the study. Animals were sacrificed for histological analyses at the end of postnatal week 16. A second group of animals received identical surgeries at week 6 and were used in a survival study. In this study mice were sacrificed only when they became recumbent.

Treatment groups

Efficacy Study: Mice were randomly divided into four groups. Group 1 consisted of transgenic mice receiving bilateral injections of CERE-120 (AAV2-NTN) into the striatum (NTN-Tg; $n=8$). Group 2 consisted of transgenic mice receiving identical injections of AAV2-enhanced green fluorescent protein (eGFP; GFP-Tg; $n=7$). Group 3 consisted of transgenic mice receiving bilateral intrastriatal injections of the vector vehicle (1X PBS with 2 mM magnesium chloride; Vehicle) that was used to formulate and dilute the vector (Veh-Tg; $n=9$). Age-matched wild-type littermates in Group 4 received intrastriatal vehicle injections (Veh-Wt; $n=11$).

Survival Study: Mice were placed into groups identical to those described above ($n=12$ in each group). All animals were treated at week 6 before the onset of behavioral symptoms.

Construction of adeno-associated viral vector

For all experiments, we used the CERE-120 (AAV2-NTN) vector, an adeno-associated viral vector type 2 (AAV2)-based gene delivery system, to administer NTN. A similar vector expressing eGFP served as a control. The structure of the AAV2 vector used is indicated in Fig. 1B. The AAV2 vector is non-pathogenic and incapable of replication. All viral coding sequences were removed, leaving behind only the non-coding inverted terminal repeats of the AAV2. The coding sequences were replaced by a NTN expression cassette consisting of a CAG promoter, a region of cDNA encoding the β -nerve growth factor pre-pro region (ppNGF) fused to the mature region of human NTN, and the polyadenylation sequence from human growth hormone. The CAG promoter consists of a human cytomegalovirus (CMV) enhancer, the chicken β -actin gene promoter and splice donor, and a rabbit β -globin gene splice acceptor. The ppNGF acts to promote processing and secretion of NTN. The AAV2-eGFP vector is identical to the AAV2-NTN vector except that the ppNGF-NTN cDNA is replaced by an eGFP cDNA. All vectors were produced in human embryonic kidney (HEK) 293 cells using the calcium phosphate triple plasmid transfection method

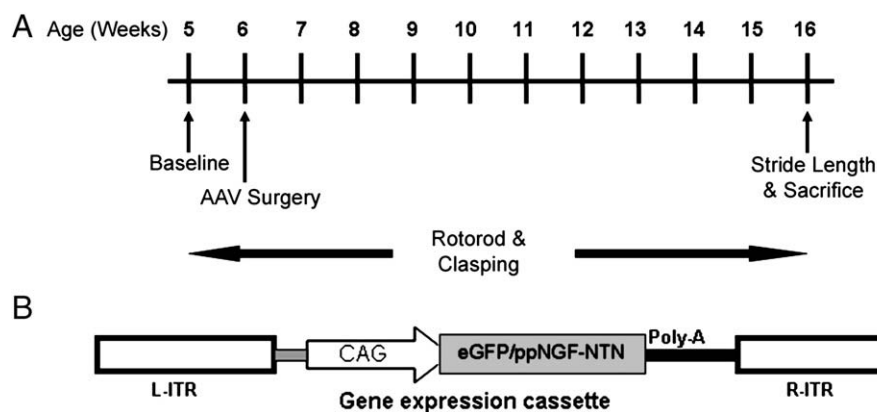


Fig. 1. (A) Timeline of Experimentation. Mice underwent baseline testing on the rotorod and claspings tests at postnatal week 5. One week later they received bilateral vector or vehicle injections into the striatum. Subsequent behavioral tests were conducted weekly until the end of the study. Hind limb stride length was measured at postnatal week 16. Animals were sacrificed for histological analyses at the end of post-natal week 16. (B) AAV2 Vector Construct. An adeno-associated viral vector type 2 (AAV-2)-based gene delivery system was used to administer NTN and eGFP. The AAV2 vector is made non-pathogenic and incapable of replication by removing all coding sequences and leaving behind only the non-coding inverted terminal repeats of the AAV2. In the AAV2-NTN (Cere-120) vector the coding sequences were replaced by a CAG promoter, a region of cDNA encoding the β -nerve growth factor pre-pro region (ppNGF) fused to the mature region of human NTN, and the polyA sequence from human growth hormone. The CAG promoter consists of a human cytomegalovirus (CMV) enhancer, a chicken β -actin promoter and splice donor, and a rabbit β -globin splice acceptor. The ppNGF acts to promote processing and secretion of NTN. The AAV2-eGFP vector is identical to the AAV2-NTN vector except that the ppNGF-NTN cDNA is replaced by an eGFP cDNA.

(Gasmi et al., 2007). Three days post transfection, cells were harvested and lysed. The AAV2 vector was purified from the cell lysates by heparin and ion exchange column chromatography. Purified particles were concentrated by centrifugal filtration and vector titer (vg/ml) was determined by Q-PCR. All vectors were created by Ceregene Inc., San Diego, CA.

Delivery of viral vector

Animals were anesthetized with a Ketamine (100 mg/kg) and Xylazine (10 mg/kg) mixture (0.1 ml/10 g i.p. per mouse) and placed in a stereotaxic frame. A midline incision was made over the skull and burr holes were drilled bilaterally above the striatum. Using a motorized injector (Stoelting) AAV2-NTN (1×10^{12} vg/ml), AAV2-eGFP (1×10^{12} vg/ml) or vehicle were infused into the striatum bilaterally (coordinates from Bregma, A/P=+0.86, M/L=±1.8, D/V=-2.85). Injections were performed using a 10 μ l Hamilton syringe with 30 gauge needles. Hamilton syringe/needle infusion systems used for vector injections were primed 20 times with the appropriate diluted vector at the beginning of each day. Prior to each injection the needles were additionally primed 20 times with the diluted vector. Injections were performed at a rate of 0.2 μ l/min. All injections were made in a 2 μ l volume. The needle was left in place for an additional 5 min to allow diffusion of the vector from the needle tip. The mice were returned to their cage and kept at a steady temperature using a heating pad.

Behavioral tests

Baseline levels of performance were determined at 5 weeks of age, prior to the vector surgeries. Subsequently, tests were performed on a weekly basis until the end of the study at post-natal week 16. Hind-limb stride length measurements were measured at week 16.

Accelerating Rotorod test

Locomotor coordination was tested using an accelerating speed rotorod (SDI, San Diego, CA) twice a week. The mice were placed on a rod of 3.2 cm diameter at a height of 45.7 cm and allowed to acclimate for 10 s. The rotorod was then turned on and accelerated at 0.1 r.p.m./s for 5 min attaining a maximum speed of 30 r.p.m. When the mice fell, a photobeam was broken, stopping a timer. The animal's latency to fall was recorded. A total of three trials were performed per testing day with 1 h between each trial. Mean weekly scores for each animal were used for statistical analysis.

Hind-limb clasping

Transgenic mice, when suspended by the tail, pull their hindlimbs together towards their body, or "clasp", a behavior not exhibited by wild type animals. To assess behavioral phenotype, mice were observed for hindlimb clasping behavior twice a week. Mice were suspended by their tail for 30 s. Mice that exhibited clasping of their hind limbs were given a score of 1 and mice that did not clasp were given a score of 0. The number of mice in each group that exhibit clasping behavior each week was noted and percentages were compared between groups.

Stride length analysis

Reduced stride length is used as an index of basal ganglia dysfunction. Stride length was measured using a protocol previously described (Fernagut et al., 2002). The hind-limbs of mice were painted using black ink. The mice were then placed in a long and narrow runway and allowed to walk on a strip of paper. Stride length was measured as the distance between identical points on two paw-prints

(Fig. 2). Measurements were averaged from four stride lengths in each run. Paw-prints made at the beginning and end of the runs were excluded from measurements. The average stride length was compared between groups.

Preparation of tissue for analysis

Efficacy study: At the end of postnatal week 16, mice were deeply anesthetized with a Ketamine (100 mg/kg) and Xylazine (10 mg/kg) mixture and sacrificed by cardiac perfusion with 100 ml 0.9% cold saline, followed by 200 ml Zamboni's fixative with 4% paraformaldehyde. Mice were decapitated, the brains removed, and post-fixed in Zamboni's fixative for 2 h. Brains were then transferred to 30% sucrose at 4 °C until completely saturated. Brains were sliced into serial coronal sections (40 μ m each) using a microtome and stored in cryoprotectant at -20 °C in 6 sets separated by 180 μ m.

Survival Study: When mice became recumbent they were deeply anesthetized with a Ketamine (100 mg/kg) and Xylazine (10 mg/kg) mixture and sacrificed by cardiac perfusion similar to animals in the efficacy study. Brains were also processed similarly for histological evaluation.

Immunohistochemistry

Efficacy study: One series of sections each were immunohistochemically labeled for NeuN (1:1000, Chemicon), NTN (1:1000, R&D Systems) or eGFP (1:4000, Abcam) using the biotin-labeled antibody procedure. Additionally, a half series of sections were labeled for mutant huntingtin (EM48; 1:300, Chemicon). Following rinsing in a Tris buffered saline (TBS) solution-containing triton-X, endogenous peroxidase activity was removed by incubation in 0.1M sodium periodate in TBS for 20 min. Non-specific background staining was blocked by incubation in Tris-containing 5% normal serum, and 0.05% triton-X for 1 h. Sections were then incubated with the appropriate

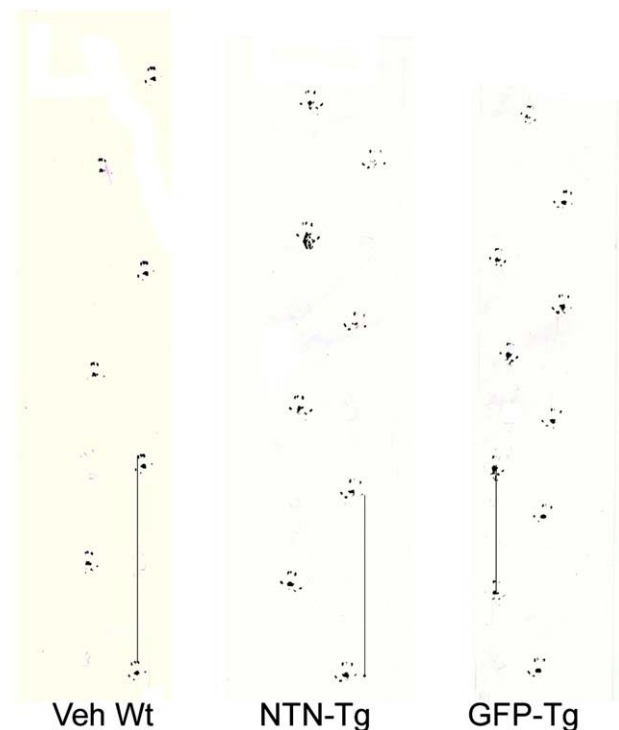


Fig. 2. Measurement of Stride length: The hind-limbs of mice were painted using black ink and mice were allowed to walk on a strip of paper placed in a long and narrow runway. Stride length was measured as the distance between identical points on two paw-prints (as indicated by lines).

primary antibody for 48 h at 4 °C. After thorough rinsing, sections were incubated with the appropriate biotinylated secondary antibody (1:200, Vector Laboratories) for 1 h. Sections were then incubated in TBS solution-containing triton-X and an ABC reagent (1:500, Vector Laboratories) for 5 min. The reaction was completed using a chromogenic solution containing 0.5% 3'3 diaminobenzidine and 0.05% hydrogen peroxide. Controls consisted of processing the tissue in an identical manner except the primary antibody solvent was employed in lieu of the primary antibody.

Survival study: One series of sections each were immunohistochemically labeled for either NTN (1:1000, R&D Systems) or eGFP (1:4000, Abcam) using the biotin-labeled antibody procedure. Additionally, a half series of sections were labeled for the mutant huntingtin antibody (EM48; 1:300, Chemicon).

Stereology

Estimates of the number of NeuN-immunoreactive (NeuN-ir) cells were performed using a design based unbiased stereological procedure. The microscope was equipped with a camera, motorized stage, and StereoInvestigator software (Microbrightfield, NJ). Estimates of NeuN-immunoreactive (NeuN-ir) cells were quantified in the striatum and frontal cortex of sections equispaced 240 μ m apart. Estimates of mutant huntingtin positive (mHtt+) cells were also quantified in the striatum of serial sections equispaced 480 μ m apart. Striatal and cortical cell counts were conducted in six serial sections that were located rostral to the anterior commissure. Similarly, three serial sections spaced 480 μ m apart, rostral to the anterior commissure and containing AAV2 vector gene product expression in the striatum were

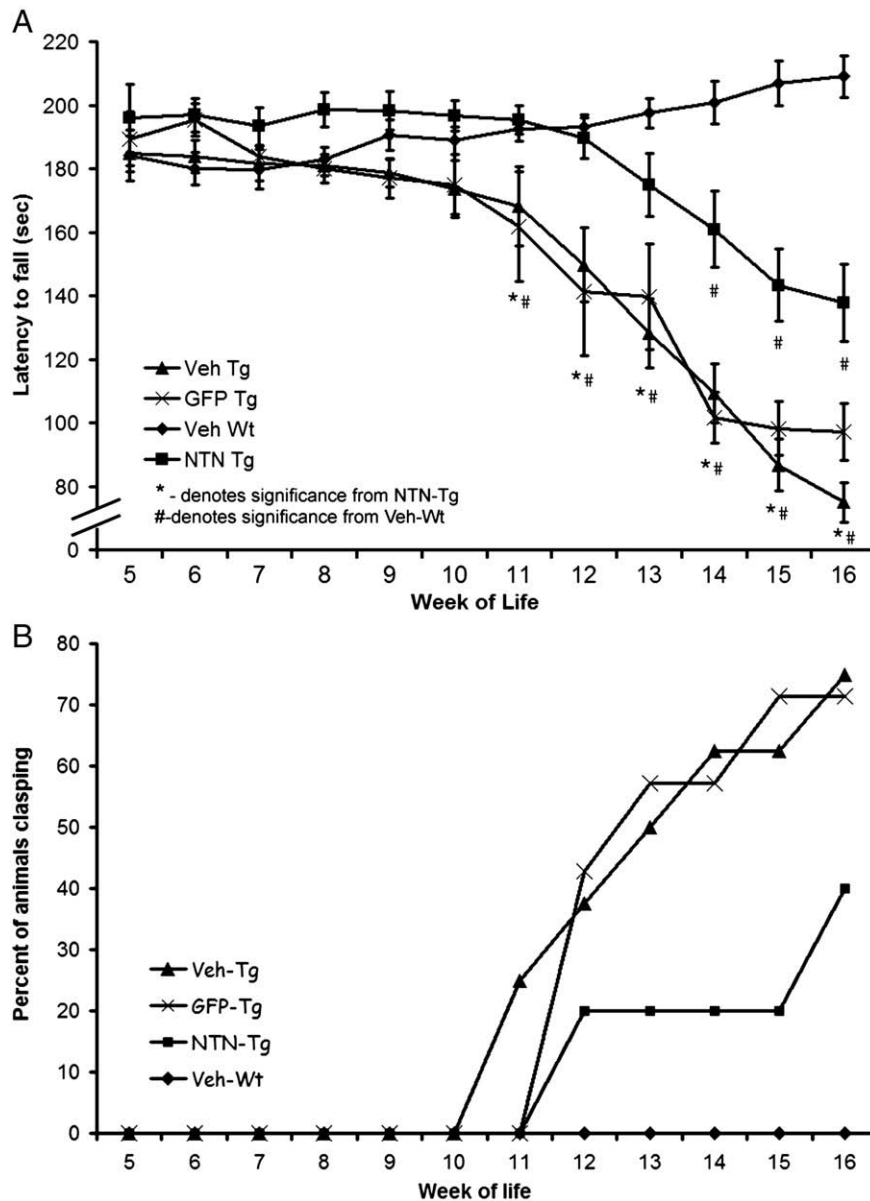


Fig. 3. (A) Rotorod: The rotorod tested balance and coordination using an accelerating paradigm. Mice in all groups performed similarly at the beginning of the study. Wild-type mice performed stably throughout the study. The performance of transgenic mice declined as the study progressed. GFP-Tg and Veh-Tg mice were significantly impaired relative to the wild-type mice. However, there was no significant difference in rotorod performance between wild-type mice and the NTN-Tg group. NTN treatment delayed decline on this task until week 13 as compared to GFP-Tg and Veh-Tg mice who declined on weeks 11 and 12 respectively. NTN-Tg mice performed significantly better than mice in both the GFP-Tg and the Veh-Tg groups starting at week 11 and continuing through week 16. (B) Clasping: Clasping is a phenotype only exhibited by transgenic mice. Veh-Wt mice never clasp. GFP-Tg and Veh-Tg groups began clasping at week 11 and 12 respectively. In both of these control groups more mice exhibited clasping behavior than mice in the Veh-Wt control group. NTN-Tg mice began to clasp at the same time as their control treated counterparts but significantly fewer mice in this group exhibited this phenotype. By week 16 only 40% of NTN-Tg mice exhibited clasping behavior compared with 71.4% of GFP-Tg-treated and 75% of Veh-Tg-treated mice.

chosen for mHtt+ cell counts. For striatal counts of either NeuN+ and mHtt+ cells, the entire striatum was first traced at 4× magnification and counts were performed under oil immersion at 100× magnification using an objective with a 1.4 numerical aperture. Similarly, cell counts were conducted in the frontal cortex in layers II–III and in layers V–VI. Layers II–III of the frontal cortex were traced at 4× magnification and then counts were performed at 100× magnification. At this higher magnification, the section thickness was empirically determined in three separate areas and an average thickness was obtained. In this regard, the stage was moved until the top of the section came into focus and the stage was zeroed at the z axis. The stage was then moved through the z axis until the bottom of the section was in focus. This yielded an average section thickness of $12 \pm 1.1 \mu\text{m}$. All cells that fell within an optical dissector height of $6 \mu\text{m}$ were counted allowing for a guard zone of $2 \mu\text{m}$ from the section top and at least 3 mm from the section bottom. Similarly layers 5 and 6 were traced and counted.

Cell volume estimates

At the same time that the optical fractionator was being employed to estimate the number of NeuN+ cells, the nucleator method was used to quantify the volume of each NeuN-ir cell that was identified in the counting frame in both the striatum and layers 5 and 6 of the cortex. A marker was placed in the center of each cell, and 5 equispaced rays extended out in a radial fashion. The computer mouse was then used to click on each point where the rays intersected the edge of the cell body. The Stereo Investigator software extrapolated the cell volume.

Statistical analyses

For the rotorod data, average weekly scores for each group were compared using a two-way repeated measures analysis of variance (ANOVA). Upon a significant interaction, multiple comparisons were made using the Student–Newman–Keuls post-hoc test. For clasping behavior, weekly percentages were compared using a one-way ANOVA on ranks and multiple comparisons were performed using a Dunn's post-hoc analysis. For stride length, right and left hind-limb stride lengths were compared using a one-way ANOVA and when a lack of significance was observed both measurements were averaged. The average hind-limb stride length was then compared between groups using a one-way ANOVA and a Student–Newman–Keuls post-hoc test. For cell counts and optical density, a one-way ANOVA was used to determine differences between cell counts in the right and left striata. When a lack of difference was established ($p > 0.05$), data from both hemispheres were averaged and a one-way ANOVA was used to compare group differences followed by a Student–Newman–Keuls post-hoc test.

Results

Rotorod

To test the effect of CERE-120 (AAV2-NTN) on balance and coordination, mice were tested on an accelerating rotorod. A repeated measures ANOVA revealed significant effects of group ($F(3,31) = 24.152$; $p < 0.001$), time ($F(11,31) = 50.244$; $p < 0.001$) and of group by time interaction ($F(33) = 14.131$; $p < 0.001$). Mice in all groups performed similarly at the first time points tested ($p > 0.05$; Fig. 3A). The performance of wild-type mice was stable and did not decline. However, as control-treated transgenic mice aged, they showed a progressive decline in performance. GFP-Tg and Veh-Tg mice showed significant deficits in balance and coordination ($p < 0.001$) relative to wild-type mice. These significant deficits were observed beginning week 11 and continued for the duration of the study. In contrast, when

the repeated measures ANOVA compared Wt mice to NTN-Tg mice over the entire time-course, there was no significant difference in rotorod performance ($p = 0.257$). However, individual post-hoc tests revealed that NTN-tg mice were impaired relative to Wt mice starting at week 14 and continuing for the duration of the study (each $p < 0.05$). NTN treatment appeared to delay decline as NTN-Tg mice did not show impairments until week 14 compared to GFP-Tg and Veh-Tg mice who declined on weeks 11 and 12, respectively. Importantly, transgenic mice receiving NTN performed significantly better than mice in both the GFP-Tg ($p < 0.05$) and the Veh-Tg ($p < 0.05$) groups starting at week 11 and continuing through the end of the testing period.

Clasping

To test the effects of CERE-120 (AAV2-NTN) on the behavioral phenotype of N171-82Q transgenic mice, clasping behavior was determined. A one-way ANOVA on ranks revealed a significant difference in clasping performance between groups ($F(2) = 4.783$; $p = 0.025$). Since Veh-Wt mice never clasped this group was not used in the statistical analysis. Both GFP-Tg and Veh-Tg groups showed similar performances to each other ($p > 0.05$) and began clasping at about week 11. Transgenic mice receiving AAV2-NTN began to clasp at the same time as their control treated counterparts but significantly fewer mice in this group exhibited clasping behavior relative to GFP-Tg and Veh-Tg mice ($p < 0.05$, Fig. 3B). In this regard, transgenic mice in all groups began clasping at similar time-points (Veh-Tg: week 11; GFP-Tg and NTN-Tg: week 12). However by week 16 only 40% of NTN-Tg mice exhibited clasping behavior compared with 71.4% of GFP-Tg-treated and 75% of Veh-Tg-treated mice.

Stride length

The stride length test was used as an index of striatal function (Table 1). A one-way ANOVA revealed a significant difference in stride length between groups ($F(3,31) = 31.469$; $p < 0.001$). Veh-Wt mice had the longest stride length. Both GFP-Tg and Veh-Tg groups had similar stride lengths to each other ($p > 0.05$) and had significantly smaller strides compared Veh-Wt animals ($p < 0.05$). In this regard, the GFP-Tg group showed a 26.8% decrease in stride length and the Veh-Tg group showed a 25.2% decrease compared to the Veh-Wt group. NTN-Tg mice took significantly longer strides than both transgenic control groups ($p < 0.05$). However the performance of this group was not completely restored relative to the Veh-Wt group as NTN-Tg mice still showed a 16.7% decrease in stride length ($p < 0.05$).

Survival data

CERE-120 (AAV2-NTN) did not prolong survival in N171-82Q transgenic mice. This transgenic model has life-spans between 2.5 and 6 months of age. NTN-Tg mice did not have prolonged survival compared to GFP-Tg and Veh-Tg mice.

Table 1
Hind-limb stride length

	Mean (cms)	SEM	
Veh-Tg	5.99	0.087	* significantly smaller than Wt
GFP-Tg	5.87	0.226	* significantly smaller than Wt
NTN-Tg	6.677	0.196	# partial attenuation
Veh-Wt	8.012	0.101	

Stride length performance tests specifically for basal ganglia dysfunction. Veh-Wt mice had the longest hind-limb stride length. Both GFP-Tg and Veh-Tg groups had significantly shorter stride lengths. NTN-Tg mice had an attenuation of stride length dysfunction and this group took significantly longer strides compared to both transgenic control groups. However AAV2-NTN treatment did not return the performance of NTN-Tg mice to that seen in the Veh-Tg groups.

NTN and eGFP gene expression

To examine transgene expression of either NTN or eGFP, sections were immunohistochemically stained for these proteins (Fig. 4). In all animals, there was robust NTN and eGFP staining in the striatum of both NTN-Tg and GFP-Tg mice respectively (Figs. 4A, B). Both fibers and cell bodies in the striatum showed positive staining for the appropriate transgene (Figs. 4C, D). In addition to the striatum, both proteins were observed within cell bodies of the substantia nigra pars compacta and fibers of the globus pallidus, entopeduncular nucleus and substantia nigra pars reticulata (Figs. 4E, F). Since eGFP is not a secreted protein, its presence in the cell bodies of the substantia nigra pars compacta suggests that there may be retrograde transport of the AAV2 vector itself to this non-injected locus, while staining in fibers of

the pars reticulata suggests anterograde transport of the eGFP protein within transduced striatonigral neurons. In Veh-Tg, GFP-Tg and Veh-Wt mice, there was no detectable NTN-ir, indicating no endogenous upregulation of NTN due to the transgenic expression of mHtt or due to a host response following intrastriatal microinjections. Additionally, there was no immunohistochemically detectable expression of NTN in the cortex of injected mice.

NeuN-ir cell counts and volume in the striatum

We have previously demonstrated that untreated N171-82Q transgenic mice display degeneration and death of NeuN-ir neurons in the striatum (McBride et al., 2006). Compared to the striata of Veh-Wt mice (Fig. 5A), the striata of transgenic mice display uniform

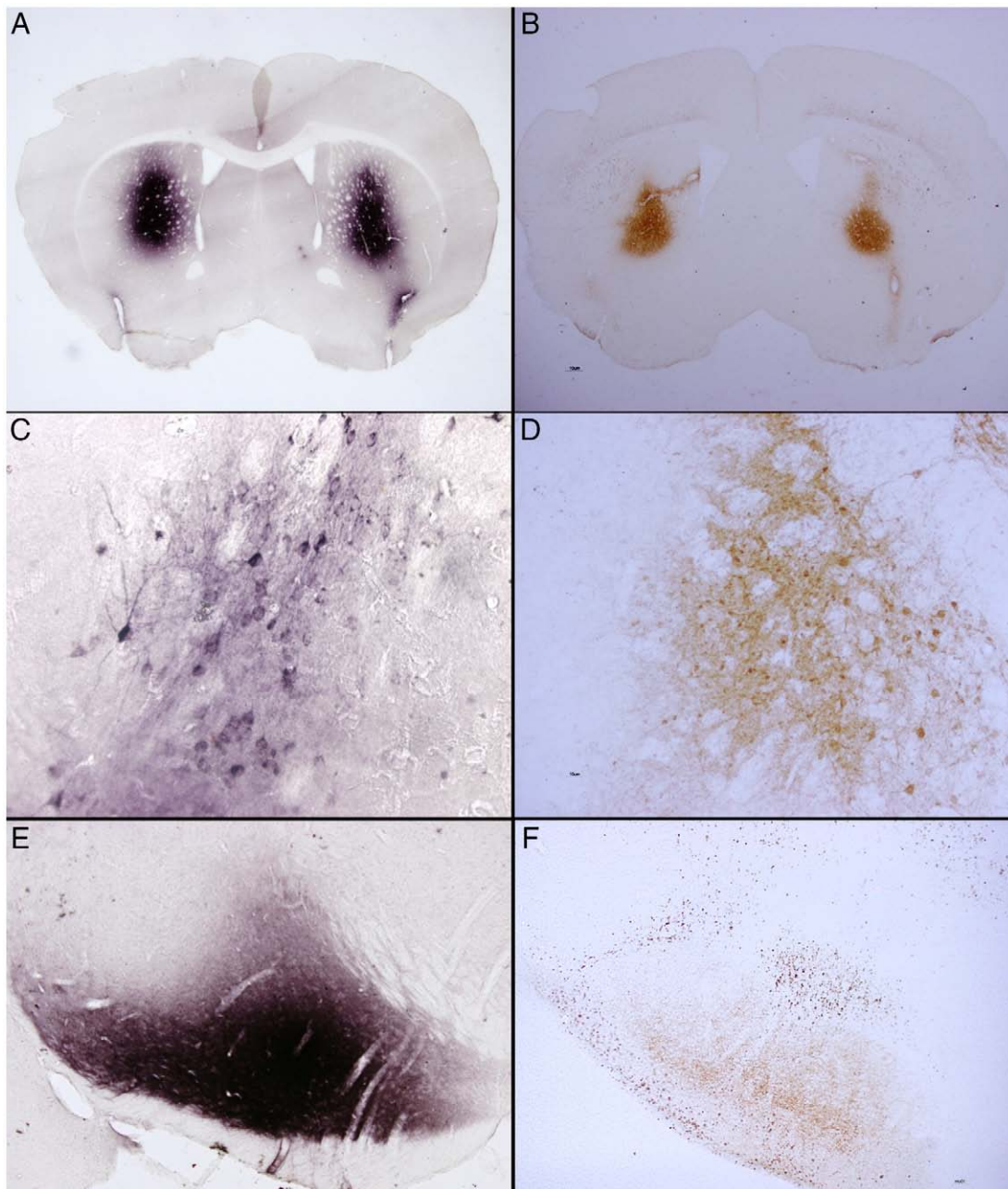


Fig. 4. Transgene expression. Robust NTN (A) and eGFP (B) staining were seen in the striatum of both NTN-Tg and GFP-Tg mice respectively. (C, D) Both fibers and cell bodies in the striatum showed positive staining for the appropriate transgene. (E, F) In addition to the striatum, both proteins were observed within cell bodies of the substantia nigra pars compacta and fibers of the globus pallidus, entopeduncular nucleus and substantia nigra pars reticulata. In Veh-Tg, GFP-Tg and Veh-Wt mice, there was no detectable NTN-ir, indicating no endogenous upregulation of NTN due to the transgenic expression of mHtt or due to a host response following intrastriatal microinjections.

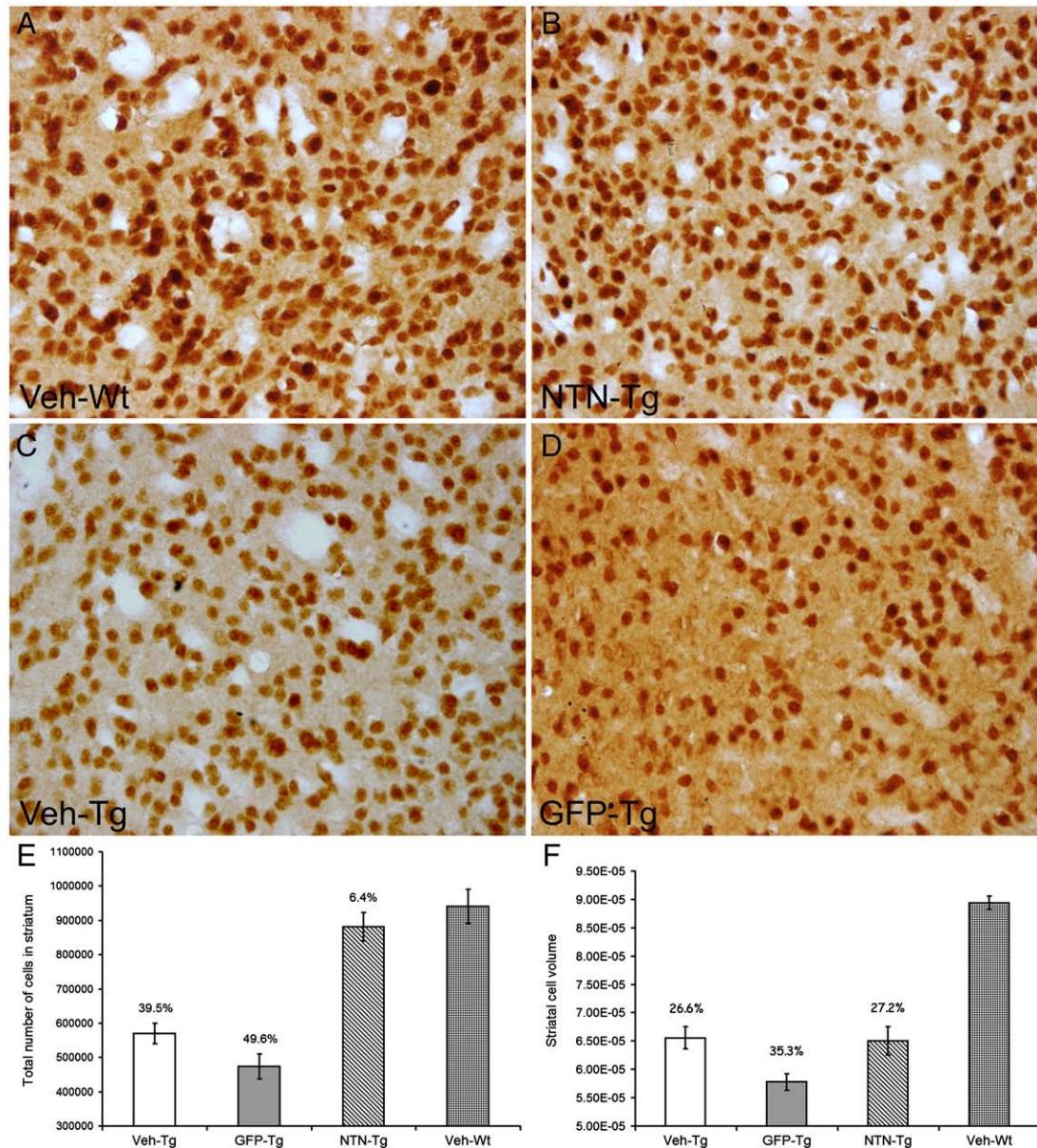


Fig. 5. Striatal cell counts and volume. (A) Image (20X) of normal cell density seen in the Veh-Wt group. (C, D) The striata of transgenic mice display uniform, widespread cell loss that is apparent at low magnification. (B) In contrast, NTN-Tg mice appear to have relatively normal densities of NeuN-ir neurons in the striatum. (E) Veh-Wt mice have a normal cell density of $9.41 \times 10^5 \pm 47,541$ (mean \pm SEM) cells. GFP-Tg and Veh-Tg groups show an average of $4.73 \times 10^5 \pm 33,366$ and $5.69 \times 10^5 \pm 27,847$ cells in the striatum respectively which is a significant cell loss compared to the Veh-Wt group. NTN-Tg mice average $8.81 \times 10^5 \pm 16,102$ cells in the striatum, a significant neuroprotection compared to both the GFP-Tg and Veh-Tg groups. Furthermore, this degree of cell loss is not significantly different from wild-type controls. (F) Using the nucleator method NeuN-ir striatal cell volume was also estimated. Normal cell volume in wild-type mice is $8.94 \times 10^{-5} \pm 1.2 \times 10^{-6}$ (mean \pm SEM). Significant decreases in cell volume are seen in the GFP-Tg and Veh-Tg groups which show an average of $5.78 \times 10^{-5} \pm 1.5 \times 10^{-6}$ and $6.56 \times 10^{-5} \pm 1.9 \times 10^{-6}$ respectively. Similarly, NTN-Tg mice have a significant decrease in cell volume relative to wild-type controls ($6.50 \times 10^{-5} \pm 2.5 \times 10^{-6}$).

widespread cell losses (Figs. 5C and D). Qualitatively, the density of NeuN-ir neurons in the striata of NTN-Tg mice appeared normal (Fig. 5B). In the present study, a one-way ANOVA revealed a significant difference in the number of cells between groups ($F(3,31)=31.213$; $p<0.001$; Fig. 5E). We first determined that there were no significant differences in NeuN-ir cell number between the right and left striata ($p>0.05$) in transgenic animals and these numbers were averaged for all four groups and then compared between groups. Wild-type mice had on average $9.41 \times 10^5 \pm 47,541$ (mean \pm SEM) cells. Estimates of NeuN-ir cell number in the GFP-Tg and Veh-Tg groups showed an average of $4.73 \times 10^5 \pm 33,366$ and $5.69 \times 10^5 \pm 27,847$ NeuN-ir neurons in the striatum, respectively. These numbers represent a 49.6% cell loss in the GFP-Tg group and a 39.5% loss in the Veh-Tg group, both of which reflect significant reductions in cell number compared to the

wild-type mice. In contrast, NTN-Tg mice averaged $8.81 \times 10^5 \pm 16,102$ cells in the striatum. This 6.4% cell loss in NTN-Tg group is significantly less than what is seen in either the GFP-Tg and Veh-Tg groups ($p<0.001$). Furthermore, this degree of cell loss is not significantly different from wild-type controls ($p=0.276$).

In addition to cell number, we also determined the influence of NTN gene delivery on striatal NeuN-ir cell volume using the nucleator method. A one-way ANOVA revealed a significant difference in the volume of individual striatal cells between groups ($F(3,31)=70.689$; $p<0.001$; Fig. 5F). Wild-type mice had an average cell volume of $8.94 \times 10^{-5} \pm 1.2 \times 10^{-6}$ (mean \pm SEM). Estimates of cell volume in the GFP-Tg and Veh-Tg groups showed an average of $5.78 \times 10^{-5} \pm 1.5 \times 10^{-6}$ and $6.56 \times 10^{-5} \pm 1.9 \times 10^{-6}$. These numbers represent a significant 35.3% decrease in the GFP-Tg group and a significant 26.6% decrease in

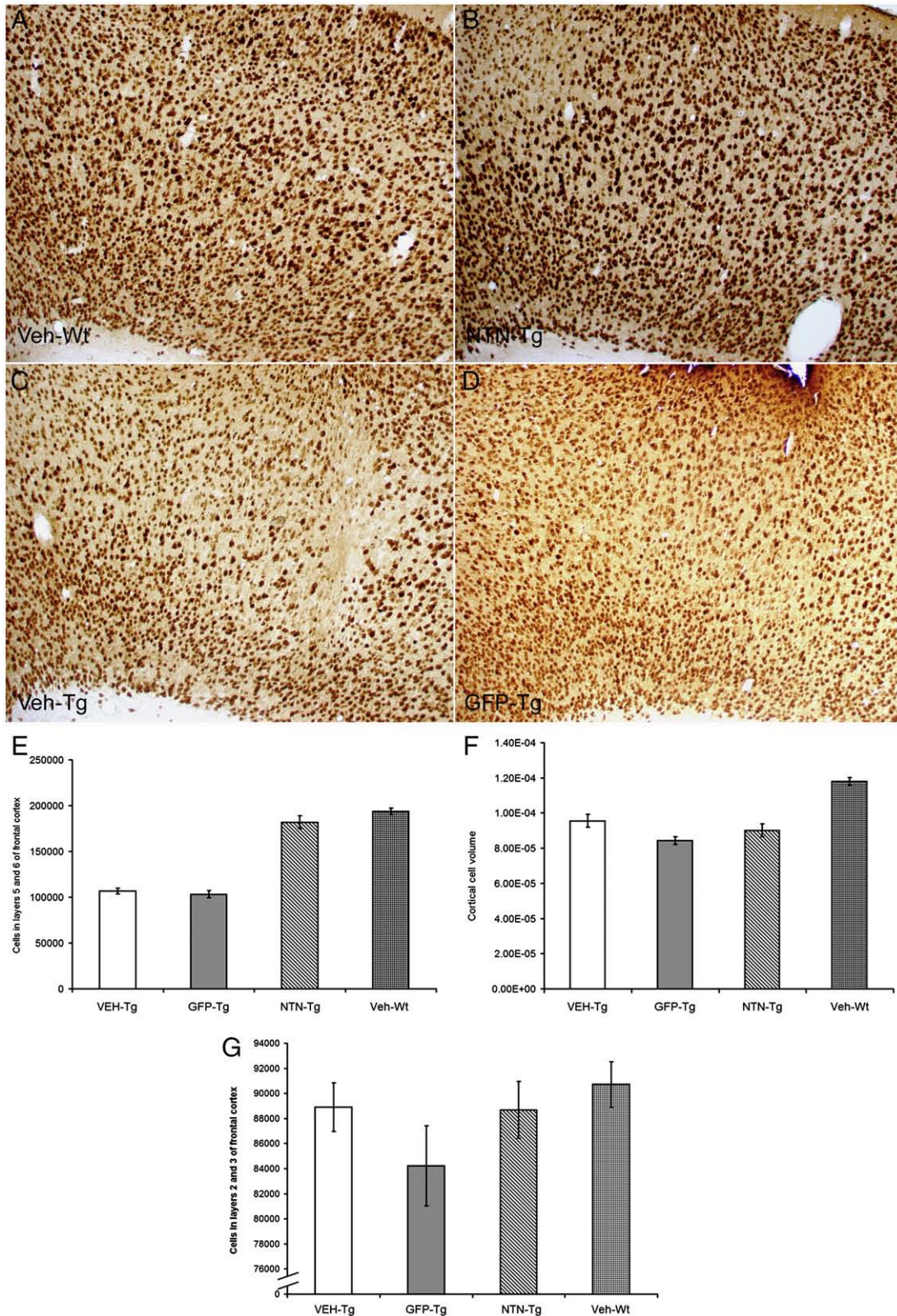


Fig. 6. Frontal cortex layers 5 and 6 cell. (A) Image (20×) of normal cell density seen in the Veh-Wt group. (B) In contrast, NTN-Tg mice seem to have an apparent sparing of NeuN-ir neurons in this region. (C, D) Layers 5 and 6 of the frontal cortex of transgenic mice displays uniform, widespread cell loss. (E) Normal cell density in layers 5/6 of the cortex in the Veh-Wt group is $1.94 \times 10^5 \pm 3,587$ (mean ± SEM) cells. Estimates of cell number in the GFP-Tg and Veh-Tg groups showed an average of $1.03 \times 10^5 \pm 3,691$ and $1.07 \times 10^5 \pm 2,996$ cells in the frontal cortex respectively which was a significant cell loss compared to the Veh-Wt group. NTN-Tg mice averaged $1.82 \times 10^5 \pm 7,090$ cells in the frontal cortex a significant neuroprotection compared to both the GFP-Tg and Veh-Tg groups. Furthermore, this degree of cell loss is not significantly different from wild-type controls. (F) Using the nucleator method cortical cell volume was also estimated. Normal cell volume in wild-type mice was of $1.2 \times 10^{-4} \pm 2.3 \times 10^{-6}$ (mean ± SEM). Significant decreases in cell volume were seen in the GFP-Tg and Veh-Tg groups which showed an average of $8.4 \times 10^{-5} \pm 2.2 \times 10^{-6}$ and $9.6 \times 10^{-5} \pm 3.7 \times 10^{-6}$ respectively. Similarly, NTN-Tg mice had a significant decrease in cell volume relative to wild-type controls ($9.0 \times 10^{-5} \pm 3.7 \times 10^{-6}$). (G) Frontal cortex layers 2 and 3 cells counts. Layers 2 and 3 of the frontal cortex do not show significant cell loss in this transgenic model.

cell volume in the Veh-Tg group relative to wild-type mice. Similarly, NTN-Tg mice averaged a cell volume of $6.50 \times 10^{-5} \pm 2.5 \times 10^{-6}$ which also represents a significant 27.2% decrease relative to wild-type controls. Cell volume estimates in the striatum of the NTN-Tg group did not differ from that seen in the GFP-Tg or Veh-Tg group ($p=0.996$).

NeuN-ir cell counts and volume in the frontal cortex

This study is the first to perform a stereological analysis of cortical NeuN-ir cell loss in N171-82Q transgenic mice. Here, we have estimated the number of NeuN-ir neurons in the frontal cortex, a region heavily impacted in HD. Combined counts were conducted in layers V–VI and also in layers II–III to compare whether cortical pathology exists in these mice similar to that seen in HD patients, and additionally to see if NTN prevented cortical cell loss.

Compared to normal cell densities seen in Veh-Wt mice (Fig. 6A), layers V–VI of the frontal cortex of transgenic mice display overt, widespread cell loss (Figs. 6C, D). This cell loss is not always uniformly distributed and some transgenic mice display large areas in which NeuN-ir neurons are completely absent. However, NTN-Tg mice appear to have normal cell densities (Fig. 6B). Overall cells appear significantly shrunken in all transgenic groups compared to cells in wild-type mice. Statistical analyses revealed no significant difference in the number of NeuN-ir neurons between left and right hemispheres in each group ($p>0.05$). These numbers were averaged for each group and then compared between groups. A one-way ANOVA on ranks revealed a significant difference in the number of cells between groups ($H(3)=24.921$; $p<0.001$; Fig. 6E). Wild-type mice had on average $1.94 \times 10^5 \pm 3587$ (mean \pm SEM) cells. Estimates of NeuN-ir cell number in the GFP-Tg and Veh-Tg groups showed an average of $1.03 \times 10^5 \pm 3691$ and $1.07 \times 10^5 \pm 2996$ cells respectively. These numbers represent a 46.7% cell loss in the GFP-Tg group and a 45% loss in the Veh-Tg group, both of which reflect significant reductions in cell number compared to the wild-type mice. In contrast, NTN-Tg mice averaged $1.82 \times 10^5 \pm 7090$ NeuN-ir neurons in the cortex. The NTN-Tg group had significantly higher numbers of cells when compared to the GFP-Tg and Veh-Tg groups ($p<0.05$). The number of cortical cells in the NTN-Tg mice represents a non-significant 6.2% loss of NeuN-ir neurons relative to wild-type controls.

To determine whether the preservation of layer V–VI cortical cells was accompanied by the preservation of cell volume, the nucleator method was employed to compare cellular volumes between groups. A one-way ANOVA revealed a significant difference in the volume of individual cortical cells between groups ($F(3,31)=23.973$; $p<0.001$; Fig. 6F). Wild-type mice had an average cell volume of $1.2 \times 10^{-4} \pm 2.3 \times 10^{-6}$ (mean \pm SEM). Estimates of cell volume in the GFP-Tg and Veh-Tg groups showed an average of $8.4 \times 10^{-5} \pm 2.2 \times 10^{-6}$ and $9.6 \times 10^{-5} \pm 3.7 \times 10^{-6}$ respectively which represents a 28.5% decrease in the GFP-Tg group and a 23.4% decrease in cell volume in the Veh-Tg group, both of which reflect a significant decrease compared to the wild-type mice. NTN-Tg mice averaged a cell volume of $9.0 \times 10^{-5} \pm 3.7 \times 10^{-6}$ which represents a 23.6% decrease relative to wild-type controls. Cell volume estimates in the cortex of the NTN-Tg group did not differ from that seen in the GFP-Tg ($p=0.58$) or the Veh-Tg ($p=0.60$) groups.

NeuN-ir neurons in layers II–III were also examined. These layers did not show a significant reduction in number ($p=0.260$, Fig. 6G). Qualitatively, there was an apparent reduction in cell volume (not quantified) indicating cellular atrophy.

Mutant huntingtin positive cells in the striatum

N171-82Q transgenic mice contain mutant huntingtin protein positive (mHtt+) inclusions in many regions of the brain. Statistical analyses determined that there was no significant difference between

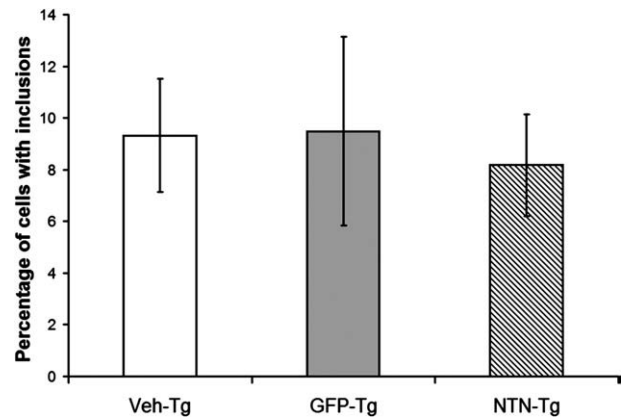


Fig. 7. Mutant huntingtin positive (mHtt+) cells in the striatum. Wild-type mice contain no mHtt+ inclusions and this group was omitted from comparison. Transgenic mice contain several mHtt+ inclusions in the striatum. Estimates of inclusion positive cell number in the GFP-Tg and Veh-Tg groups showed an average of $4.0 \times 10^4 \pm 14,486$ and $5.6 \times 10^4 \pm 16,560$ cells in the striatum respectively. NTN-Tg mice averaged $7.4 \times 10^4 \pm 18,230$ mHtt-positive cells in the striatum. Although this indicates an increase in raw mHtt+ counts in the striatum, this group also contained a significantly larger number of NeuN-ir neurons in this region of the brain. Therefore, this graph indicates the percentage of striatal cells that contained inclusions. The difference found between groups was non-significant with 9.5% of cells in GFP-Tg, 9.3% of cells in Veh-Tg and 8.2% of cells in NTN-Tg mice containing mHtt+ inclusions.

the number of mHtt+ cells between hemispheres ($p>0.05$) and these numbers were averaged for each group. Since wild-type animals do not contain mHtt positive inclusions, no counts were conducted for this group and these animals were not included in the analysis. A one-way ANOVA revealed no significant difference in the number of mHtt+ cells between groups ($F(2,20)=1.024$; $p=0.377$). Estimates of inclusion positive cell number in the GFP-Tg and Veh-Tg groups showed an average of $4.0 \times 10^4 \pm 14,486$ and $5.6 \times 10^4 \pm 16,560$ cells in the striatum respectively. NTN-Tg mice averaged $7.4 \times 10^4 \pm 18,230$ mHtt-positive cells in the striatum. This increase in the raw number of mHtt+ cells in mice receiving NTN gene delivery likely reflects the enhanced NeuN-ir cell survival seen in this group. Therefore, we also estimated the percentage of striatal cells that contained inclusions. This calculation was conducted by dividing the number of mHtt+ cells by the total number of NeuN-ir neurons and multiplying by 100. The difference found between groups was non-significant ($F(2,20)=0.0778$; $p=0.925$; Fig. 7) with 9.5% of cells in GFP-Tg, 9.3% of cells in Veh-Tg and 8.2% of cells in NTN-Tg mice containing mHtt+ inclusions.

Discussion

This study is the first to show, that CERE-120 (AAV2-NTN) gene transfer administered prior to the onset of symptoms in the N171-82Q transgenic HD mouse model provides both functional and structural neuroprotection. We found that NTN delivery could delay the development and lessen the severity of behavioral deficits and prevent NeuN-ir cell loss in the striatum. Critically, this is the first study to show that intrastriatal delivery of AAV2-NTN protects and prevents cell loss in the frontal cortex, a brain region significantly affected in HD and one that likely underlies the cognitive symptoms suffered by HD victims, considered by many to be the most devastating of the disease. In the well established transgenic N171-82Q mouse model of HD (Schilling et al., 1999) mice develop symptoms relatively later than other transgenic mouse models starting at around 2.5 months of age (McBride et al., 2006). This models an adult onset of symptoms. Additionally, similar to HD patients, mice have shortened lifespans, motor deficits and NeuN-ir cell loss within the striatum and the cortex.

In order to determine whether improvements in behavioral phenotypes correlated with neuroprotection, NeuN-ir cell counts

were conducted in both the striatum and the cortex. CERE-120 (AAV2-NTN) administration to the striatum completely ameliorated cell loss that was seen in GFP-Tg and Veh-Tg controls. There was no significant difference between the total numbers of cells seen in wild-type controls compared to NTN-treated controls. It is notable that there was a tendency for the GFP-Tg group to have greater cell loss than the Veh-Tg group suggesting that some minor toxicity from GFP might have been involved. Previous studies using AAV2-GDNF in this mouse model of HD have also shown promising results. [McBride et al. \(2006\)](#) demonstrated that AAV2-GDNF, when administered prior to the onset of symptoms, prevents significant NeuN-ir cell loss in the striatum. That study showed that, compared to wild-type mice, the AAV2-GDNF group had only an 8% cell loss in the striatum compared with the transgenic control groups that showed a 22% loss. Our results with AAV2-NTN were comparable, if not superior to those seen with GDNF. A second study comparing fibroblasts transfected with either a neurturin cDNA or a GDNF cDNA showed that NTN specifically protected striatal projection neurons and GDNF protected both projection neurons and interneurons in a toxin model of HD ([Perez-Navarro et al., 2000](#)). Since striatal projection neurons are more severely affected in HD patients compared to interneurons ([Ferrante et al., 1987](#)), the aforementioned study supports the concept that neurturin has potential as a therapy in patients.

We also examined individual cell volume within the striatum. These results were less promising as all transgenic mice including those receiving NTN showed a significant reduction in cell volume compared to wild-types. This indicates that although AAV2-NTN completely protects NeuN-ir neurons from cell death there is still some cellular atrophy associated with disease progression that is not ameliorated.

One of the most exciting findings in this study is that CERE-120 (AAV2-NTN) administration to the striatum also completely protected NeuN-ir neurons in layers 5 and 6 of the frontal/prefrontal cortex. Layers V–VI were chosen because numerous studies have shown that HD patients experience the most cell loss in these layers of the frontal cortex ([Hedreen et al., 1991](#); [Selemon et al., 2004](#)). In this mouse model we see a significant loss of NeuN-ir neurons in layers 5 and 6 but not in layers II–III. This dissociation is interesting as layers V–VI are the cells of origin for corticostriate connections while layers II–III are the cells of origin for corticocortical connections. These data suggest that the preservation of the striatum played a role in the preservation of the cortex. Interestingly, AAV2-NTN was only administered to the striatum and there was no detectable retrograde transport of NTN from the striatum to the cortex, using immunohistochemical methods. Our hypothesis is that by protecting cells within the striatum, factors independent of NTN are secreted which then influence the viability of cortical neurons. This bystander effect has been seen in other systems where it can produce either positive or negative outcomes. Implantation of polymer encapsulated fibroblasts genetically engineered to secrete CNTF into the striatum of non-human primates, prior to an excitotoxic lesion, can prevent the loss of striatal neurons and also the retrograde atrophy of neurons in layer V of the cortex ([Emerich et al., 1997b](#)). A negative bystander effect has been seen in the cortical ablation model, in which factors such as calpain are released that causes secondary cell loss in other regions. Studies have shown that by blocking these calpains secondary degeneration can be reduced in areas that are anatomically connected to the lesioned site ([Bartus et al., 1999](#)). It is possible that protecting striatal cells and having intact afferent and efferent connections is enough to protect cortical cells that might have otherwise undergone a secondary degeneration. Although, it is important to note that in HD patients, cortical loss can sometimes precede striatal loss. Cell loss within the cortex of patients is likely responsible for cognitive deficits such as impairments in executive function, psychomotor skills and procedural memory tasks. Additionally, it is likely that the severe personality changes displayed by HD patients are cortically mediated. The ability of CERE-120 (AAV2-

NTN) to protect NeuN-ir cortical cells may ultimately translate into preventing the cognitive and personality deficits seen in animal models as well as patients.

Similar to HD patients, N171-82Q transgenic mice have large numbers of mHtt-positive inclusions in many regions of the brain including the striatum. The expanded polyglutamine stretch in mutant huntingtin confers upon the protein a toxic gain of function. While the mechanism of mutant huntingtin induced toxicity is controversial, several hypotheses involving the formation of cytoplasmic inclusions have been advanced. Large cytoplasmic inclusions formed by the aggregation of mutant huntingtin may be toxic to the cell ([Waelter et al., 2001](#)). Furthermore huntingtin aggregates can sequester proteins that are essential for cell viability and survival. Aggregates have been shown to recruit transcription factors ([Perez et al., 1998](#)), caspases ([Sanchez et al., 1999](#)) and protein kinases ([Meriin et al., 2001](#)). Huntingtin aggregates can also sequester CREB-binding protein, a major player in cell survival, and prevent its function ([Nucifora, et al., 2001](#)). Thus by sequestering and inhibiting the function of otherwise viable proteins, mutant huntingtin aggregates can retard the efficient functioning of otherwise normal neurons. However, other prevailing theories suggest that aggregation of mutant huntingtin may actually be neuroprotective since it sequesters the damaged protein and prevents it from causing widespread damage to the cell. This hypothesis is supported by data showing that non-aggregated mutant huntingtin can also cause cell death ([Saudou et al., 1998](#)). In order to determine whether CERE-120 (AAV2-NTN) elicits its neuroprotective effects by altering the number of inclusions within the striatum, we counted cells in the striatum that contained inclusions. Our results indicated that AAV2-NTN did not alter the number or percentage of cells that contain mHtt-positive inclusions. This suggests that AAV2-NTN induced neuroprotection does not depend on altering inclusion number within the striatum and that significant prevention of behavioral abnormalities can be achieved despite a heavy inclusion load, which is promising for patients at more advanced disease states. It is interesting to note that AAV2-GDNF treatment, as shown previously by our lab, decreases the percentage of cells in the striatum that have mHtt+ inclusions ([McBride et al., 2006](#)). While both AAV2-NTN and AAV2-GDNF have similar effects on NeuN-ir neuronal protection, the evidence that AAV2-GDNF also reduces mHtt+ cells indicates a possible difference in mechanism of action between both neurotrophic factors.

In the present study we determined whether neuroprotection conferred improvements in functional behavior. We have shown that viral delivery of NTN in a mouse model of HD results in the delay of symptom development and lessening of symptom severity. These improvements may be accounted for by the protection of NeuN-ir striatal cells observed in this group, as rotorod performance is partially dependent on striatal function. CERE-120 (AAV2-NTN) administration also decreased the probability of hind-limb claspings in transgenic mice. While it is unclear which brain regions are involved in this behavior, NTN's ability to alter claspings phenotype may be due to striatal or cortical neuroprotection. Although NTN administration prior to the onset of symptoms does not completely ameliorate the onset of behavioral symptoms, results obtained are still very encouraging. Most HD patients develop some sign of the disease between the ages of 30 and 50 and worsening of symptoms continues for many years. These devastating symptoms include chorea, bradykinesia, severe weight loss, sleep disturbances, memory loss, depression, mania and suicidal tendencies. Thus, the symptoms are not only limited to motor domains but include cognitive and psychiatric disturbances. While the most ideal therapy would completely ameliorate symptomology, even delaying the onset of symptoms or their rate of progression would be of great benefit to HD patients.

Unfortunately, CERE-120 (AAV2-NTN) did not prolong lifespan in this model. Other systemic approaches like Coenzyme Q10 and remacemide ([Ferrante et al., 2002](#)) and lipoic acid ([Andreassen et al.,](#)

2001) are able to improve survival in this model. The fact that we were not able to extend survival with our localized therapy, despite significant cellular sparing in the striatum and cortex, raises the hypothesis that HD pathology outside of the striatum or cortex must be the cause of death in this model. In fact, the leading causes of death in HD patients are pneumonia and cardiovascular disease (Lanska et al., 1988). Therefore a multi-system approach in addition to AAV2-NTN may be necessary to extend survival in patients.

This study supports the concept that NTN is neuroprotective in rodent models of HD. We demonstrate in the present study, that delivery of NTN using an AAV2 vector provides widespread gene delivery within the striatum and prevents striatal NeuN-ir cell death and associated behavioral pathology. While these results indicate that AAV2-NTN is efficacious when administered prior to the onset of symptoms, it is important to test whether positive results could be achieved when administered after symptom onset. Together with the present results, those data would provide important empirical support for the concept of testing AAV2-NTN to determine whether it might be useful as a novel treatment for some of the major pathology and symptoms of HD.

Acknowledgments

The funding for this project was from the Hope for Huntington's Foundation and a generous donation from the Fiori Family. CDH, JHK, MG, and RTN have a financial interest in Ceregene Inc.

References

- Anderson, K.D., Panayotatos, N., Corcoran, T.L., Lindsay, R.M., Wiegand, S.J., 1996. Ciliary neurotrophic factor protects striatal output neurons in an animal model of Huntington disease. *Proc. Natl. Acad. Sci. U. S. A.* 93, 7346–7351.
- Andreassen, O.A., Ferrante, R.J., Dedeoglu, A., Beal, M.F., 2001. Lipoic acid improves survival in transgenic mouse models of Huntington's disease. *NeuroReport* 12, 3371–3373.
- Bartus, R.T., Chen, E.Y., Lynch, G., Kordower, J.H., 1999. Cortical ablation induces a spreading calcium-dependent, secondary pathogenesis which can be reduced by inhibiting calpain. *Exp. Neurol.* 155, 315–326.
- Canals, J.M., Pineda, J.R., Torres-Peraza, J.F., Bosch, M., Martin-Ibanez, R., Munoz, M.T., Mengod, G., Ernfors, P., Alberch, J., 2004. Brain-derived neurotrophic factor regulates the onset and severity of motor dysfunction associated with enkephalinergic neuronal degeneration in Huntington's disease. *J. Neurosci.* 24, 7727–7739.
- Emerich, D.F., Cain, C.K., Greco, C., Saydoff, J.A., Hu, Z.Y., Liu, H., Lindner, M.D., 1997a. Cellular delivery of human CNTF prevents motor and cognitive dysfunction in a rodent model of Huntington's disease. *Cell Transplant* 6, 249–266.
- Emerich, D.F., Winn, S.R., Hantraye, P.M., Peschanski, M., Chen, E.Y., Chu, Y., McDermott, P., Baetge, E.E., Kordower, J.H., 1997b. Protective effect of encapsulated cells producing neurotrophic factor CNTF in a monkey model of Huntington's disease. *Nature* 386, 395–399.
- Fernagut, P.O., Diguets, E., Labattu, B., Tison, F., 2002. A simple method to measure stride length as an index of nigrostriatal dysfunction in mice. *J. Neurosci. Methods* 113, 123–130.
- Ferrante, R.J., Kowall, N.W., Beal, M.F., Martin, J.B., Bird, E.D., Richardson Jr., E.P., 1987. Morphologic and histochemical characteristics of a spared subset of striatal neurons in Huntington's disease. *J. Neuropathol. Exp. Neurol.* 46, 12–27.
- Ferrante, R.J., Andreassen, O.A., Dedeoglu, A., Ferrante, K.L., Jenkins, B.G., Hersch, S.M., Beal, M.F., 2002. Therapeutic effects of coenzyme Q10 and remacemide in transgenic mouse models of Huntington's disease. *J. Neurosci.* 22, 1592–1599.
- Gasmi, M., Herzog, C.D., Brandon, E.P., Cunningham, J.J., Ramirez, G.A., Ketchum, E.T., Bartus, R.T., 2007. Striatal delivery of neurturin by CER-120, an AAV2 vector for the treatment of dopaminergic neuron degeneration in Parkinson's disease. *Molec. Ther.* 15, 62–68.
- Hedreen, J.C., Peyser, C.E., Folstein, S.E., Ross, C.A., 1991. Neuronal loss in layers V and VI of cerebral cortex in Huntington's disease. *Neurosci. Lett.* 133, 257–261.
- Lanska, D.J., Lavine, L., Lanska, M.J., Schoenberg, B.S., 1988. Huntington's disease mortality in the United States. *Neurology* 38, 769–772.
- Marks Jr., W.J., Ostrem, J.L., Verhagen, L., Starr, P.A., Larson, P.S., Bakay, R.A., Taylor, R., Cahn-Weiner, D.A., Stoessl, A.J., Olanow, C.W., Bartus, R.T., 2008. Safety and tolerability of intraputamin delivery of CER-120 (adeno-associated virus serotype 2-neurturin) to patients with idiopathic Parkinson's disease: an open-label, phase 1 trial. *Lancet Neurol.* 7, 400–408.
- Martinez-Serrano, A., Bjorklund, A., 1996. Protection of the neostriatum against excitotoxic damage by neurotrophin-producing, genetically modified neural stem cells. *J. Neurosci.* 16, 4604–4616.
- McBride, J.L., Ramaswamy, S., Gasmi, M., Bartus, R.T., Herzog, C.D., Brandon, E.P., Zhou, L., Pitzer, M.R., Berry-Kravis, E.M., Kordower, J.H., 2006. Viral delivery of glial cell line-derived neurotrophic factor improves behavior and protects striatal neurons in a mouse model of Huntington's disease. *Proc. Natl. Acad. Sci. U. S. A.* 103, 9345–9350.
- Meriin, A.B., Mabuchi, K., Gabai, V.L., Yaglom, J.A., Kazantsev, A., Sherman, M.Y., 2001. Intracellular aggregation of polypeptides with expanded polyglutamine domain is stimulated by stress-activated kinase MEKK1. *J. Cell Biol.* 153, 851–864.
- Nucifora Jr., F.C., Sasaki, M., Peters, M.F., Huang, H., Cooper, J.K., Yamada, M., Takahashi, H., Tsuji, S., Troncoso, J., Dawson, V.L., Dawson, T.M., Ross, C.A., 2001. Interference by huntingtin and atrophin-1 with cbp-mediated transcription leading to cellular toxicity. *Science* 291, 2423–2428.
- Perez, M.K., Paulson, H.L., Pendse, S.J., Saionz, S.J., Bonini, N.M., Pittman, R.N., 1998. Recruitment and the role of nuclear localization in polyglutamine-mediated aggregation. *J. Cell Biol.* 143, 1457–1470.
- Perez-Navarro, E., Akerud, P., Marco, S., Canals, J.M., Tolosa, E., Arenas, E., Alberch, J., 2000. Neurturin protects striatal projection neurons but not interneurons in a rat model of Huntington's disease. *Neuroscience* 98, 89–96.
- Ramaswamy, S., McBride, J.L., Herzog, C.D., Brandon, E., Gasmi, M., Bartus, R.T., Kordower, J.H., 2007. Neurturin gene therapy improves motor function and prevents death of striatal neurons in a 3-nitropropionic acid rat model of Huntington's disease. *Neurobiol. Dis.* 26, 375–384.
- Reiner, A., Albin, R.L., Anderson, K.D., D'Amato, C.J., Penney, J.B., Young, A.B., 1988. Differential loss of striatal projection neurons in Huntington disease. *Proc. Natl. Acad. Sci. U. S. A.* 85, 5733–5737.
- Sanchez, I., Xu, C.J., Juo, P., Kakizaka, A., Blenis, J., Yuan, J., 1999. Caspase-8 is required for cell death induced by expanded polyglutamine repeats. *Neuron* 22, 623–633.
- Saudou, F., Finkbeiner, S., Devys, D., Greenberg, M.E., 1998. Huntingtin acts in the nucleus to induce apoptosis but death does not correlate with the formation of intranuclear inclusions. *Cell* 95, 55–66.
- Schilling, G., Becher, M.W., Sharp, A.H., Jinnah, H.A., Duan, K., Kotzok, J.A., Slunt, H.H., Ratovitski, T., Cooper, J.K., Jenkins, N.A., Copeland, N.G., Price, D.L., Ross, C.A., Borchelt, D.R., 1999. Intranuclear inclusions and neuritic aggregates in transgenic mice expressing a mutant N-terminal fragment of huntingtin. *Hum. Mol. Genet.* 8, 397–407.
- Selemmon, L.D., Rajkowska, G., Goldman-Rakic, P.S., 2004. Evidence for progression in frontal cortical pathology in late-stage Huntington's disease. *J. Comp. Neurol.* 468, 190–204.
- The Huntington's Disease Collaborative Research Group, 1993. A novel gene containing a trinucleotide repeat that is expanded and unstable on Huntington's disease chromosomes. *Cell* 72, 971–983.
- Waelter, S., Boeddrich, A., Lurz, R., Scherzinger, E., Lueder, G., Lehrach, H., Wanker, E. E., 2001. Accumulation of mutant huntingtin fragments in aggresome-like inclusion bodies as a result of insufficient protein degradation. *Mol. Biol. Cell* 12, 1393–1407.